

Chemical disorder-induced magnetism in FeSi₂ nanoparticles

Y. Y. Chen,^{a)} P. C. Lee,^{b)} C. B. Tsai, and S. Neeleshwar^{c)}
Institute of Physics, Academia Sinica, Taipei, Taiwan 115, Republic of China

C. R. Wang
Department of Physics, Tunghai University, Taichung, Taiwan, 407, Republic of China

J. C. Ho and H. H. Hamdeh
Department of Physics, Wichita State University, Wichita, Kansas 67260, USA

(Received 25 July 2007; accepted 28 November 2007; published online 19 December 2007)

Iron disilicide in a bulk form is practically nonmagnetic. In contrast, nanoparticles of FeSi₂ exhibit superparamagnetism with blocking temperatures ranging from 8 K (15 nm) to 34 K (55 nm). Their relatively low saturation magnetization suggests that the magnetic behavior is associated with only a small fraction of Fe ions, which have a sufficient number of other Fe as nearest neighbors. The chemical disorder is presumably induced in the formation of nanoparticles. A spin glass-type anomaly below 10 K observed in specific heat data gives a further evidence for the compositional heterogeneity. © 2007 American Institute of Physics. [DOI: 10.1063/1.2825467]

For bulk Fe_xSi_{1-x}, Fe carries a magnetic moment and undergoes a ferromagnetic transition above 500 °C only if $x \geq 0.5$.¹ The equiatomic compound FeSi ($x=0.5$) exhibits a peculiar activation-type increase of magnetic susceptibility at low temperatures followed by the Curie-Weiss-like dependence above 500 K.² The anomalous behavior attracted many theoretical considerations, including the one based on the itinerant electron picture by taking into account the effects of exchange enhanced spin fluctuations.³ At a much lower Fe content with $x=0.33$, iron disilicide FeSi₂ is practically nonmagnetic.¹ FeSi₂ transforms from a metallic high-temperature α -phase to a room-temperature semiconducting β -phase at about 937 °C. The narrow-gap semiconductor β -FeSi₂ has been well recognized for potential applications in a broad range of technology from thermoelectrical devices and solar cells⁴ to optoelectronic.⁵ Considering the fast advancement of microelectronics, it becomes more important for us to understand the physical properties pertaining to nanomaterials. Of particular interest to this work on β -FeSi₂ is the realization that the synthesis process of nanoparticles can often induce large chemical disorder in lattice, which may then lead to significantly different magnetic behaviors from that of the bulk. The recent discovery in ZnFe₂O₄ of transformation from antiferromagnetism in bulk to ferrimagnetism in nanoparticles is a good example.⁶ Such a magnetic behavior created by chemical disorder in nanoparticles could enhance the potential applications of semiconducting FeSi₂ in magnetoelectronics and nanodevices.

Bulk FeSi₂ was prepared by arc melting through mixed constituent elements, Fe (99.97%) and Si (99.999%) in 1:2 atomic ratio, followed by annealing at 850 °C for 72 h to form a single phase of β -FeSi₂. The expected orthorhombic structure of the β -phase, having a primitive cell of 48 atoms containing two sets of 8 Fe each, was confirmed by x-ray diffraction (XRD) patterns in Fig. 1. The lattice parameters

($a=7.836$ Å, $b=7.796$ Å, and $c=9.866$ Å) are in good agreement with literature values.⁷

Nanoparticles were fabricated by ArF excimer laser ablation of the bulk as target. Samples of size $d=15, 22, 36, 40,$ and 55 nm, respectively, were collected on a liquid nitrogen-cooled copper plate. The particle size was basically controlled by processing parameters including the helium gas pressure (0.5–0.6 torr), the laser power (1.25–5.0 W). In general, lower gas pressure and power level generally yielded smaller particles. XRD patterns in Fig. 1 indicate that the orthorhombic structure remains the same as that of bulk compound, consistent with EDS data showing close to 1:2 ratio between Fe and Si, except the line broadening and a slight amount of Cu from cold trap in the smaller particles. Since Cu is nonmagnetic, its contribution in magnetic measurements is extremely small. Each particle size was actually determined by fitting the full width at half maximum (FWHM) of the (422) peak to a theoretical simulation⁸ in Fig. 2. Transmission electron microscopy (TEM) was employed to directly observe particle morphology and crystal-line structure. The shapes of particles are nearly spherical in Fig. 2. The average size for each specimen is in consistent

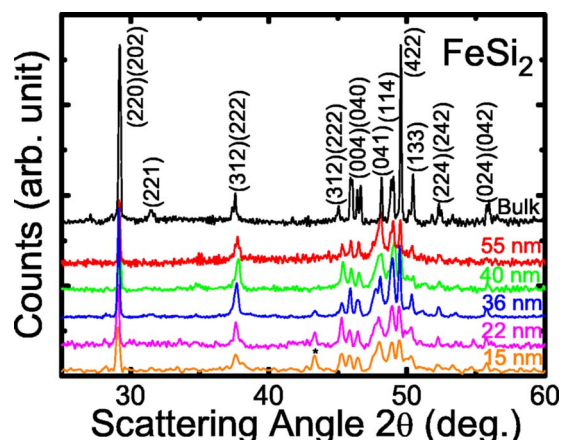


FIG. 1. (Color online) The x-ray diffraction patterns of orthorhombic bulk and nanoparticle FeSi₂. The peak with * notation is a characteristic one from copper.

^{a)}Electronic mail: chen2@phys.sinica.edu.tw.

^{b)}Also at Department of Engineering and System Science, National Tsing Hua University.

^{c)}Present address: School of Basic and Applied Science, GGS Indraprastha University, Delhi, India.

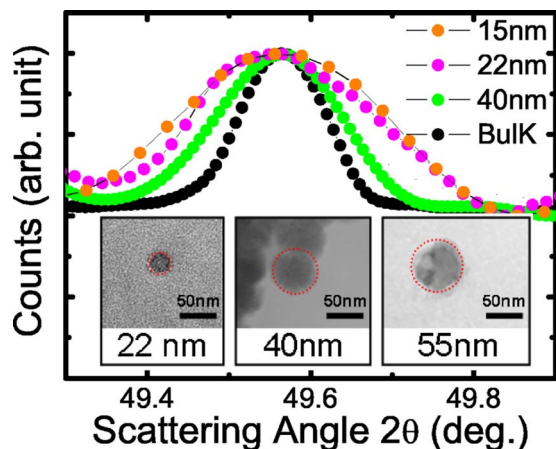


FIG. 2. (Color online) The FWHM of (422) peaks provide a measure of the nanoparticle sizes for 15, 22, 40 nm, and bulk (from top to bottom). Also shown are sample TEM images of nanoparticles.

with that obtained from XRD. The estimated standard deviation of particle size distribution is about $\pm 10\%$ of the mean value. Magnetic measurements were carried out using a Quantum Design superconducting quantum interference device (SQUID). Specific heat measurements for temperature below 30 K were carried out using a thermal-relaxation microcalorimeter.⁹

In comparison with that of bulk FeSi_2 , the magnetic susceptibilities χ of nanoparticles are greatly enhanced at ambient temperatures and below. Irreversible phenomena between field-cooling and zero-field-cooling (ZFC) curves in Fig. 3 reveal a characteristic superparamagnetism. The blocking temperature T_B is determined from the peak of each ZFC curve and plotted in Fig. 4. In terms of magnetization versus H/T , Fig. 4(a) shows an expected magnetic hysteresis at a temperature below but not above T_B . The high-field magnetization data up to 5 T at 5 K in the inset of Fig. 4 follow the equation $M = M_s(1 - \alpha/H)$, where α is a measure of magnetic hardness. The saturation magnetization obtained has relatively low values, ranging from 1330 emu/mol in 55 nm to 814 emu/mol in 40 nm and 468 emu/mol in 15 nm at 5 K. By assuming $2\mu_B$ per magnetic Fe, these M_s values correspond to only about 4%–11% (0.08 – $0.23\mu_B$) of magnetic Fe in the samples. It is most likely that certain Fe-rich chemical disorders exist. Magnetic moment and

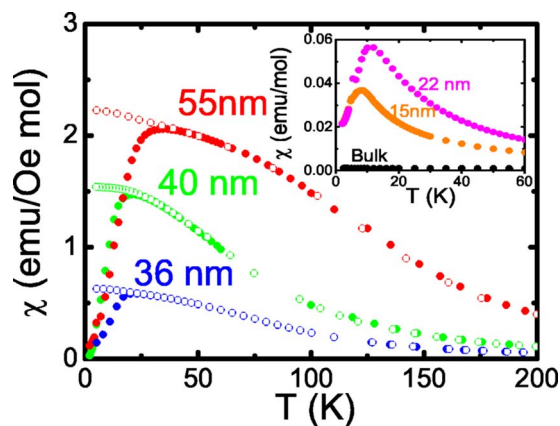


FIG. 3. (Color online) Temperature dependence of magnetic susceptibility for bulk and nanoparticle FeSi_2 . For clarity, only ZFC data are shown for samples in the inset.

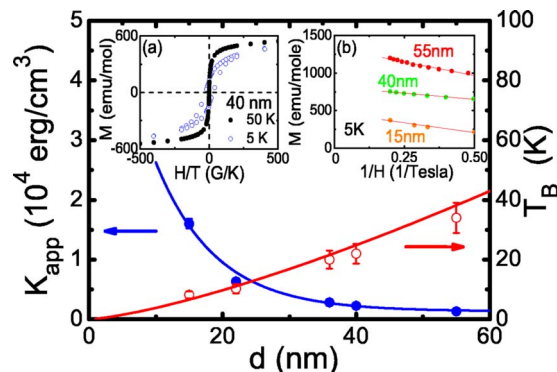


FIG. 4. (Color online) Particle-size dependence of blocking temperature and apparent anisotropic constant. (a) M - H curves for 40 nm particles ($T_B = 22$ K), showing a hysteresis at 5 K but not at 50 K. (b) High-field magnetization M vs $1/H$, fitted to the relation $M = M_s(1 - \alpha/H)$.

short-range-order would prevail as long as a given Fe is surrounded by a sufficient number of other Fe as nearest neighbors. While such a chemical disorder had been observed though Hall effect in FeSi_2 single crystals,¹⁰ it is understandably much easier to be induced in the formation of nanoparticles. A similar effect in nanoparticle ZnFe_2O_4 showing a ferrimagnetic behavior is caused by partial site exchange between Zn and Fe in a cubic spinel structure. Zinc ferrite in a bulk form is antiferromagnetic below 10 K.⁶

If K is the anisotropic constant and V is the volume of nanoparticle, then the anisotropic energy KV represents an energy barrier to the total spin reorientation for the particle. In a standard analysis for superparamagnetism,¹¹ the time constant for spin reorientation is expressed as

$$\tau = \tau_0 \exp(KV/k_B T), \quad (1)$$

where τ_0 is of the order of 10^{-9} s. However, this is meaningful only for chemically homogeneous superparamagnets. Each nanoparticle has presumably a single magnetic domain and KV represents an effective anisotropy energy barrier to the total spin reorientation for the particle. For multicluster particles, the factor V should not be the whole particle but rather the individual cluster volume. Since the actual cluster size is unknown, one can simply replace KV in Eq. (1) by an effective anisotropic energy barrier ε_{eff} . Letting the value of τ equal to 100 s corresponding approximately to the SQUID measuring time, ε_{eff} is obtained as

$$\varepsilon_{\text{eff}} = 25k_B T_B. \quad (2)$$

It ranges from 0.018 eV (15 nm) to 0.075 eV (55 nm). For intercomparison with other systems, it would still be worthwhile to come up with an “apparent” value of anisotropic constant K_{app} based on the whole particle volume V such that $K_{\text{app}} = \varepsilon_{\text{eff}}/V$. This parameter in Fig. 4 increases dramatically with decreasing particle size, in consistent with the report on nanostructured CuFe_2O_4 , for which spin-disordered structure at the interface could be the origin of the observation.¹²

Further along the same line, it is reasonable to anticipate that some very small clusters may not participate in the blocking temperature phenomenon, but exhibit a secondary effect at temperatures below. Indeed, a small magnetic susceptibility step appears for the 22 and 40 nm samples at approximately 5 K. Corroborative evidence comes from our calorimetric measurements in Fig. 5. A contribution to specific heat in addition to the lattice term has its peak shifted to

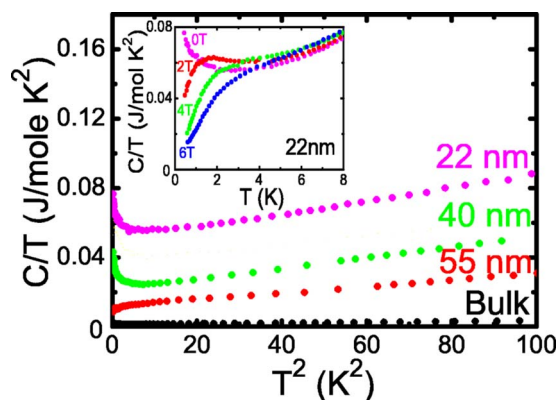


FIG. 5. (Color online) Temperature dependence of specific heat as shown in C/T vs T^2 . Inset: A low-temperature spin glass-type anomaly shifts to higher temperatures as magnetic field increases.

higher temperatures with an applied magnetic field of 2 T or above. Coupled with the Fe-rich clusters mentioned above, this anomalous effect is believed to be an indication of a spin glass-type transition associated with smaller magnetic cluster.¹³

In conclusion, in contrast to the bulk form, nanoparticles (15–55 nm) of FeSi_2 contain small fractions of Fe-rich clusters. They lead to superparamagnetism, with the blocking temperature decreasing and the apparent anisotropy constant or effective anisotropy energy increasing with decreasing particle size. A secondary effect of spin glass-type anomaly occurs near 10 K.

We are thankful for the use of the Core facilities for nanoscience and nanotechnology in Academia Sinica. This work was supported by the National Research Council, the Republic of China, under Grant No. NSC 94-2112-M-001-044.

- ¹O. Kubaschewski, *Iron-Binary Phase Diagrams* (Springer, New York 1982), p. 136.
- ²V. Jaccarino, G. K. Wertheim, J. H. Wernick, L. R. Walker, and S. Arajs, *Phys. Rev.* **160**, 476 (1967).
- ³Y. Takahashi, *J. Phys.: Condens. Matter* **10**, L671 (1998) and references therein.
- ⁴E. Müller, C. Drasar, J. Schilz, and W. A. Kaysser, *Mater. Sci. Eng., A* **362**, 17 (2003).
- ⁵D. Leong, M. Harry, J. Reeson, and K. P. Homewood, *Nature (London)* **387**, 686 (1997).
- ⁶H. H. Hamdeh, J. C. Ho, and S. A. Oliver, *J. Appl. Phys.* **81**, 1851 (1997).
- ⁷Y. Dusausoy and J. Protas, *Acta Crystallogr., Sect. B: Struct. Crystallogr. Cryst. Chem.* **27**, 1209 (1971).
- ⁸W.-H. Li, S. Y. Wu, C. C. Yang, S. K. Lai, K. C. Lee, H. L. Huang, and H. D. Yang, *Phys. Rev. Lett.* **89**, 135504 (2002).
- ⁹*Temperature: Its Measurement and Control in Science and Industry* (American Institute of Physics, New York, 2003), Vol. 7, p. 387.
- ¹⁰P. Lengsfeld, S. Brehme, G. Ehlers, H. Lange, N. Stüsser, Y. Tomm, and W. Fuhs, *Phys. Rev. B* **58**, 16154 (1998).
- ¹¹B. D. Cullity, *Introduction to Magnetic Materials* (Addison Wesley, New York, 1972), p. 410.
- ¹²J. Z. Jiang, G. F. Goya, and H. R. Rechenberg, *J. Phys.: Condens. Matter* **11**, 4063 (1999).
- ¹³E. V. Sampathkumaran, N. Mohapatra, S. Rayaprol, and K. K. Iyer, *Phys. Rev. B* **75**, 052412 (2007).